



4th IASPEI / IAEE International Symposium:

Effects of Surface Geology on Seismic Motion

August 23–26, 2011 • University of California Santa Barbara

STRONG MOTION CHARACTERISTICS AND THEIR DAMAGE IMPACT TO STRUCTURES DURING THE OFF PACIFIC COAST OF TOHOKU EARTHQUAKE OF MARCH 11, 2011; HOW EXTRAORDINARY WAS THIS M9.0 EARTHQUAKE?

Hiroshi Kawase

Disaster Prevention Research Institute
Kyoto University, Uji, Kyoto 611-0011
JAPAN

ABSTRACT

On March 11, 2011, a huge subduction zone earthquake occurred offshore of the Tohoku district, Japan, and created devastating damage, primarily due to the very high Tsunami tide along the Pacific coast. We first review several source studies and then summarize basic characteristics of observed strong motions with reference to the attenuation relationships, response spectra, linear site factors in the region, and nonlinearity seen on HVRs. The current release of K-NET and KiK-net data for the main shock from NIED consists of 697 and 518 sites, respectively, including MYG004 with the largest horizontal PGA of 2.7g and the other seventeen sites with vector-summed PGA larger than 1g. Fortunately we haven't seen heavy damage concentration close to the source region, which might extend about 500 km in length. We need to answer the question why this was the case. We calculate building damage potential of these records using the nonlinear response models derived from the damage statistics during the Hyogo-ken Nanbu earthquake of 1995. We conclude that PGAs were high because of high stress drop in the western side of the source and large site factors in high frequency range in the area but that PGVs were not high enough to make buildings heavily damaged or collapsed.

INTRODUCTION

A M9.0 mega-thrust earthquake occurred off the coast of Miyagi Prefecture ($38^{\circ}6.2'N$, $142^{\circ}51.6'E$) at 14:46:18.1 on March 11, 2011, with the hypocenter being 24 km deep based on the information released by the Japan Meteorological Agency (JMA). JMA named this earthquake "the 2011 Off the Pacific Coast of Tohoku (Tohoku-Chiho Taiheiyo-Oki) Earthquake". Since this earthquake was a low-angle reverse fault and aftershocks have been occurring along the upper surface of the subducting Pacific Plate, it was clear that the earthquake occurred on the boundary between the Pacific Plate and the North American Plate on which the Tohoku Region of Japan rests. What was surprising at was the size of the earthquake, which created unprecedented heights of Tsunamis all along the coast of Tohoku Region. This is a brief report on this earthquake and its observed strong motions, which seem to have smaller potential to structural damage despite of their quite high values of PGAs. Pervasively observed soil nonlinearity will also be briefly covered.

GENERAL INFORMATION ON THE OFF PACIFIC COAST, TOHOKU EARTHQUAKE

As mentioned above this earthquake was a low-angle reverse fault as shown by the analysis of teleseismic data in Figure 1 (JMA, 2011a). Figure 2 shows the distribution of aftershocks that occurred on March 11 (JMA, 2011b). It can be seen that the aftershocks occurred widely in the Pacific Ocean between off-Sanriku and off-Ibaraki Prefecture. The area of these immediate aftershocks suggest about 200km by 500km of the rupture area, which is about the size of M9 class earthquakes as the scaling law suggests.

Prior to this earthquake, a M7.3 earthquake occurred on August 16, 2005, off Miyagi Prefecture, west of the epicenter of the main shock. At first it was considered that this might be the recurrence of the M7.8 Off Miyagi Prefecture (Miyagi-ken Oki) earthquake that occurred on June 12, 1978, causing significant damage in Sendai City. Subsequent studies, however, showed that only about half of

the fault area ruptured during the 1978 event was ruptured at that time and the rest remained without slip. As a result of this study, the Headquarters for Earthquake Research Promotion estimated the possibility of an earthquake occurring off Miyagi Prefecture in the next 30 years at 99%.

Figure 3 shows the map of the predicted seismogenic zones (hypothesized segments) prepared prior to the occurrence of the main shock. Several experts said, based upon this map, that the earthquake occurred as a result of the coupled destruction of the Off-Central Sanriku, Off-Miyagi Prefecture, Off-Southern Sanriku, Off-Fukushima Prefecture and Off-Ibaraki Prefecture Zones; it is true, however, the segments shown in Fig. 3 assume their uncoupled behavior based on the historical records of earthquake occurrence, and this earthquake therefore raises the fundamental question whether such segmentation based on the past earthquake history over a relatively short period of time, along with the estimation of the possibility of earthquake occurrence for each segment, actually has any meaning at all or not.

In addition to the 2005 Miyagi-ken Oki earthquake on March 9, 2011, shortly before the main shock, another M7.3 earthquake occurred off Southern Sanriku area (38°19.7'N, 143°16.7'E), at the same latitude but closer to the trench axis. The hypocenter of the main shock was located between the hypocenters of these two events, which suggests that the rupture of these two areas triggered the main shock. Figure 4 shows the distribution of the aftershocks from March 9th earthquake⁴⁾. When JMA analyzed the b-value of these aftershocks after the main shock, JMA found that it was only 0.4, much smaller to the ordinary value of 0.9 to 1.0, suggesting that this was a foreshock.

SOURCE PROCESS OF THE OFF PACIFIC COAST, TOHOKU EARTHQUAKE

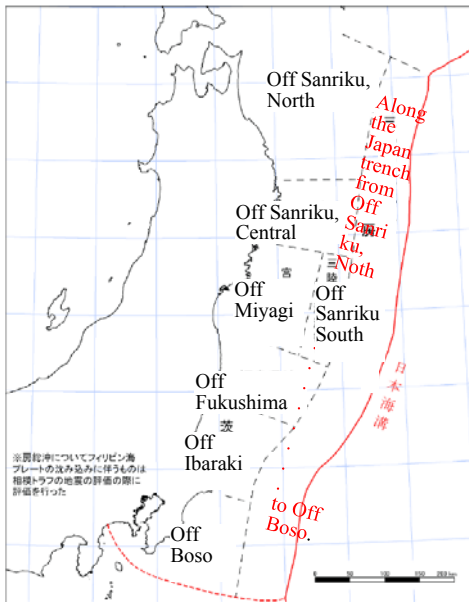


Figure 3. Assumed segments of earthquake occurrence along the Pacific Coast of the Tohoku Region (HERP, 2009).

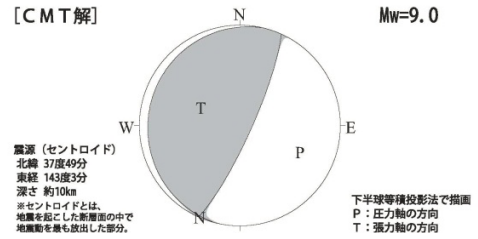


Figure 1. Mechanism solution of the Off Pacific Coast Tohoku earthquake obtained by JMA (2011a).

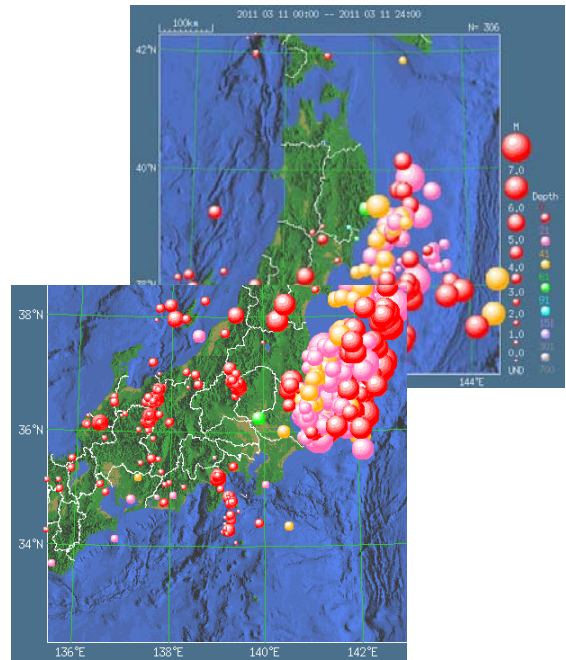


Figure 2. Aftershocks and associated earthquakes on March 11 after the Off Pacific Coast Tohoku earthquake (JMA 2011b).

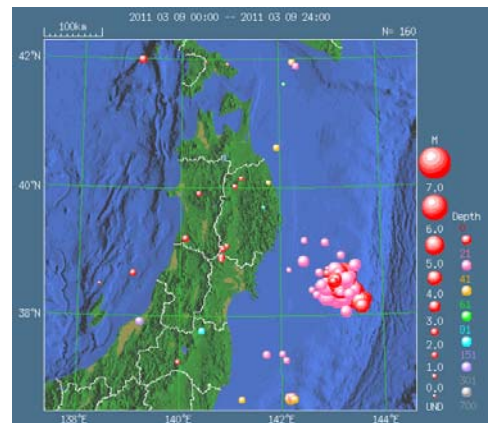


Figure 4. Aftershocks of the Sanriku-Oki earthquake of March 9, 2011.

Several research institutes determined the source process, source region, and slip distribution using teleseismic data, tectonic deformation, tsunami height and strong-motion waveforms, and so on. Limited space does not allow us to present all of the results, and so we only present here typical inversion results for different constrained conditions.

First, Figure 5 shows the crustal movement vectors (top: horizontal, bottom: vertical) determined by the Geospatial Information Authority of Japan associated with the main shock by using GPS data (GSI, 2011a). It can be seen that horizontal displacement of up to 5.3 m occurred at the tip of the Oshika Peninsula, and that the direction of the displacement was east-southeast, which is the same as the direction of the CMT slip shown in Figure 1. Displacement in the vertical direction, without exception, shows subduction on land. As a co-seismic motion this is not consistent with the fact that before the earthquake these areas are also subducting continuously due to constant movement of the Pacific Plate.

The slip distribution was obtained first by determining the distribution of static displacement for the crustal movement data shown in Figure 5. The area with high slip was found to be located near the hypocenter off Miyagi Prefecture, the maximum slip was estimated to be 24 m, and the width and lengths of the areas with great rupture were 200 km and 400 km, respectively, reaching off Fukushima Prefecture in the south, but not any farther south than that, and reaching off Central Sanriku, but not any farther north than that.

Then, the Geospatial Information Authority of Japan (GSI) performed another inversion of slip distribution, this time including the ocean crustal movement data from the Maritime Safety Agency (GSI, 2011b). The results are shown in Figure 6. It was estimated that the maximum slip near the trench was 60 m, reflecting the ocean crust movement near the hypocenter being 24 m horizontally and 3 m vertically (upward). Based on this estimation, another area with a slip of around 10 m is located between off Southern Fukushima Prefecture and off Ibaraki Prefecture.

Figure 7 shows the distribution of slip for each fault element, determined based on tsunami waveforms by Fujii and colleagues at the Building Research Institute (BRI, 2011). Since the time constant of tsunami is in the order of tens of minutes, much longer than time scale of seismic waves, it is considered that this figure shows the final slip on the fault plane at the completion of the earthquake, which is the same as static crustal movement determined by GPS. The figure shows that slip became larger toward the east of the hypocenter, the area with a slip of 15m or more was 150 km in width and 200 km in length, and that the maximum slip was over 26 m. The main rupture area was, as expected, south of Off Central Sanriku and north of Off Fukushima

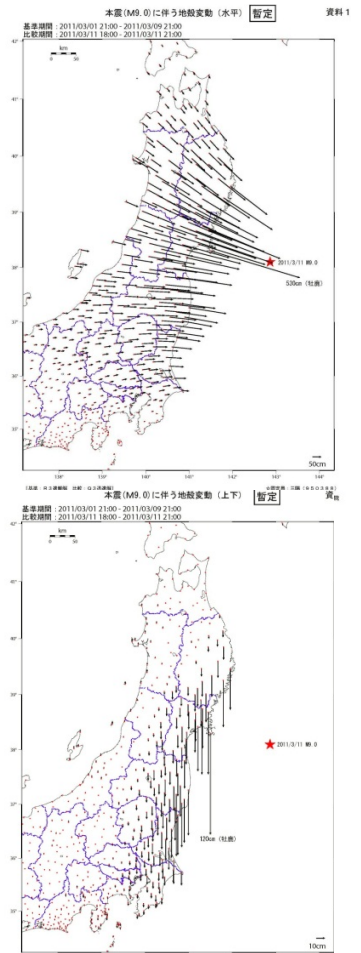


Figure 5. Crustal Movement associated with the main shock by the GPS network of GSI (2011a).

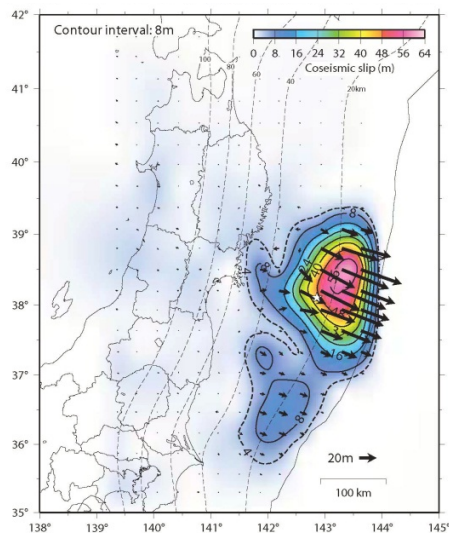


Figure 6. Static slip inverted from crustal deformation from GPS and MSA ocean bottom measurement (GSI, 2011b).

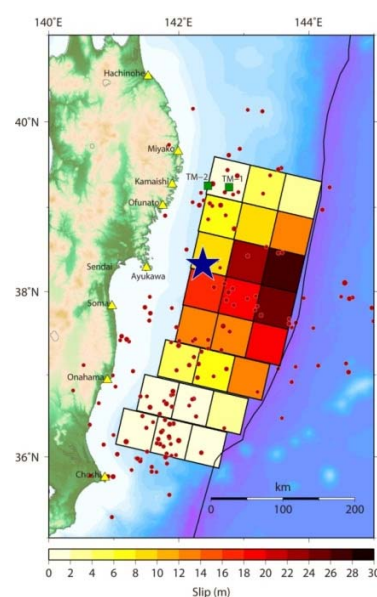


Figure 7. Slip amount inverted from tsunami waveforms (BRI,

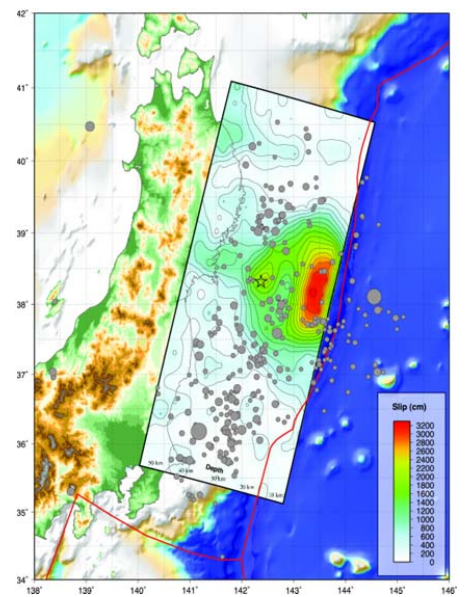


Figure 8. Slip distribution inverted from teleseismic waveforms (USGS, 2011).

Prefecture, and does not extend to Off Ibaraki Prefecture.

Figure 8 shows the distribution of slip inverted by the US Geological Survey (USGS, 2011) based on the teleseismic waveforms recorded by long-period (or broadband) seismographs located around the world. It is considered that this figure reflects the fault motion with the time constant from 20 seconds to several hundreds of seconds. This inversion from the teleseismic data also confirms the slip up to 30 m east of the hypocenter, closer to the trench, which is consistent with the results of the inversion using geodetic motions or tsunami waveforms (Figures 6 and 7). The region with a slip of 10m or more has the area of approximately 150 km × 250 km, indicating again that a large slip occurred in a relatively compact region.

The inversion of source process using observed teleseismic waveforms was conducted by not only the USGS but researchers around the world, including Japanese researchers, and with minor differences in details, a consistent result was seen of a large slip of 25–30 m occurring over 200 km to the east of the hypocenter, near the Japan Trench. Please refer to the website of the Earthquake Research Institute, The University of Tokyo, for such a comparison of several results (ERI, 2011).

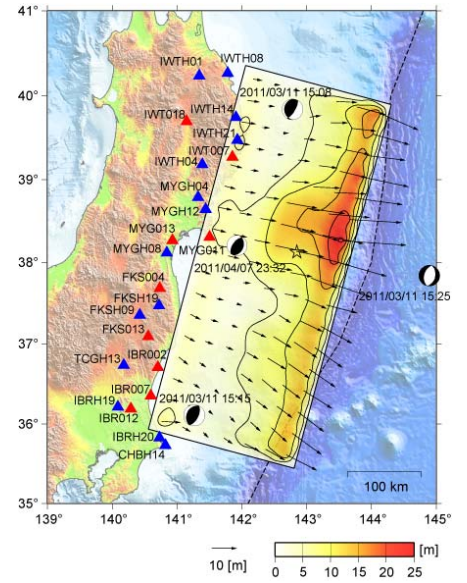


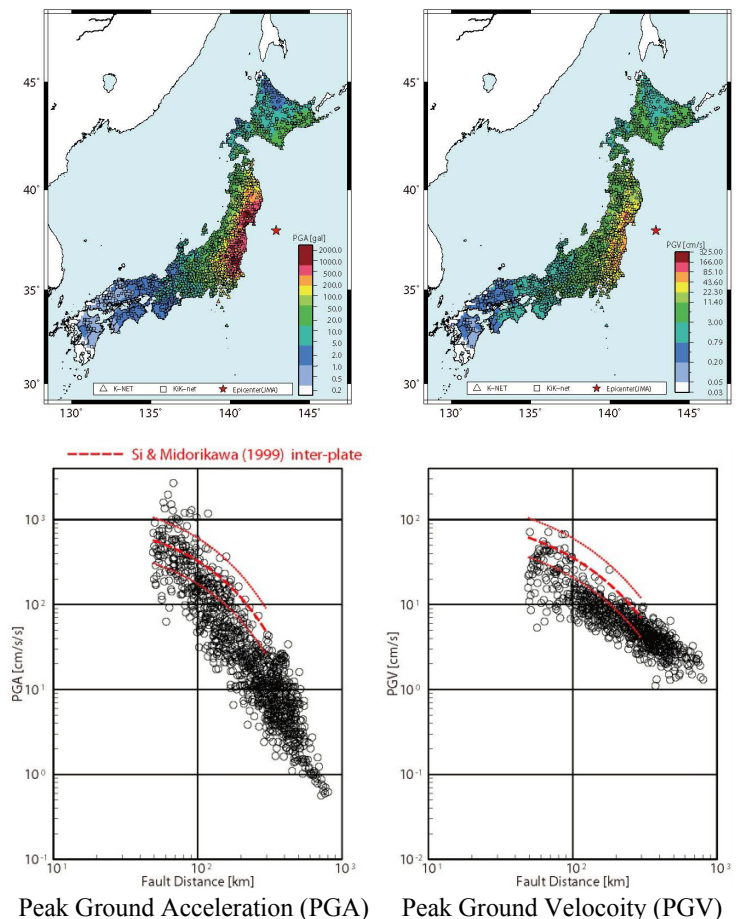
Figure 9. Slip distribution inverted from long-period strong motions from K-NET and KiK-net of NIED (NIED, 2011).

Figure 9 shows the results of the inversion, performed by Suzuki and colleagues at the National Research Institute for Earth Science and Disaster Prevention (NIED), from long-period (8 seconds or longer) strong ground motions observed by K-NET and KiK-net (NIED, 2011). The figure shows that large slips occurred near and to the east of the rupture initiation point (☆), and between Off Central Sanriku and Off Miyagi Prefecture, and that the maximum slip was 25 m, consistent with the results of the other inversions shown here. However, in these results, the region of large slip (10 m or larger) extends along the Japan trench to Off Ibaraki Prefecture. Considering that the model of static displacement including ocean crust movement produced a slip of approximately 8 m Off Ibaraki Prefecture as shown in Figure 6, it might need to be considered that rupture did indeed reach that far.

OBSERVED STRONG MOTION RECORDS

This earthquake generated a large number of strong motion records with high acceleration at many observation points, mainly in Miyagi and Ibaraki Prefectures. The distribution of seismic intensities observed or collected by JMA, which were broadcasted immediately after the main shock, shows that intensity 7 was recorded only at K-NET Tsukidate (MYG004) in Kurihara City 50km north of Sendai, but that intensity 6+ were recorded at 40 points in four prefectures.

Figure 10 shows the distribution of the peak ground acceleration (PGA) and velocity (PGV) of the strong motion records observed by K-NET and KiK-net of NIED (2011), along with the empirical attenuation relation of Shi and Midorikawa (1999) with variations (red lines). In the attenuation plot, the horizontal axis indicates the shortest distance to the rectangular fault plane shown in Figure 9. The magnitude of the event M9.0 used to calculate this attenuation was apparently extrapolation for the formula since such a large event was not included in the regression data. It can be seen PGAs exceeded 500 Gal extensively along the coast from the Central Sanriku to Ibaraki



Peak Ground Acceleration (PGA) Peak Ground Velocity (PGV)

Figure 10. Peak ground acceleration (PGA) and velocity (PGV) distributions (NIED, 2011) and their empirical attenuations of Shi and Midorikawa (1999).

Prefecture; however, PGVs in the area were lower than 80 cm/sec (except for MYG004 where PGV is around 100 cm/s), and in most areas lower than 40 cm/sec.

When compared with the attenuation formula, it seems that this earthquake produced strong motions of the average or slightly weaker level, except at points within 100 km that had higher PGAs. As previously mentioned, this earthquake was M9.0 and was one of the largest in scale in Japan's recorded history; however, the area with the largest slip was farthest from the coast, as shown in Figures 6 to 9, and therefore even if that area with longer time constant of slip also produced short-period strong motions, these seismic waves might not have contributed significantly to the sites along the coast. The area that generated short-period seismic motions and their attenuation characteristics will be discussed later.

Table 1. PGA values at the K-NET and KiK-net stations where vector-summed PGA exceeded 1g.

MYG004	Tukidate	2,700	1,268	1,880	2,933
MYG012	Shoigama	758	1,969	501	2,019
IBR003	Hitachi	1,598	1,186	1,166	1,845
MYG013	Sendai	1,517	982	290	1,808
IBR013	Hokota	1,355	1,070	811	1,762
TCG009	Imaichi	1,017	1,186	493	1,444
FKS016	Shirakawa	1,295	949	441	1,425
FKSH10	Saigo	1,062	768	1,016	1,335
IBR004	Oomiya	1,283	1,007	775	1,312
TCGH16	Haga	799	1,197	808	1,305
TCG014	Mogi	711	1,205	494	1,291
IWT010	Ichinoseki	998	852	353	1,226
IBRH11	Iwase	815	827	815	1,224
MYGH10	Yamamoto	871	853	622	1,137
FKS018	Kooriyama	745	1,069	457	1,110
FKS008	Funabiki	1,012	736	327	1,069
IBRH15	Omaeyama	606	781	640	1,062
CHB007	Sakura	1,036	491	200	1,054

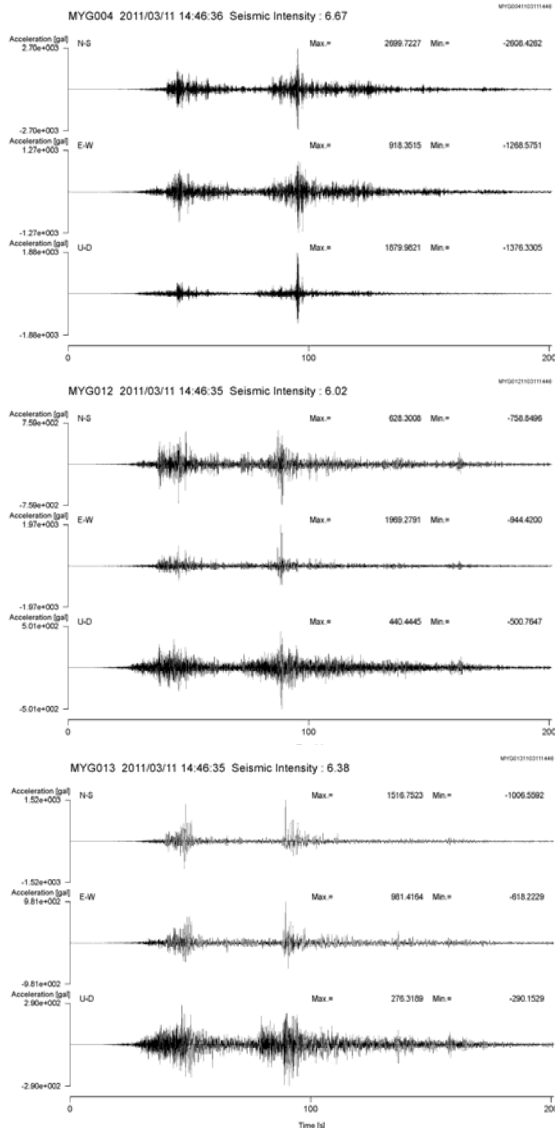


Figure 11. Accelerograms at three K-NET sites in Miyagi Prefecture (NIED, 2011).

Table 1 shows the points where the synthetic maximum acceleration of strong motions observed by K-NET and KiK-net exceeded 1 g (NIED, 2011b). While many of the sites are located in Miyagi and Fukushima Prefectures, it is notable that Tochigi and Chiba Prefectures also have such points, even though they are distant from the main source area, off Miyagi Prefecture.

Detailed discussion on individual records will not be made here, but let us examine at least three components of the acceleration waveform at three sites; at MYG004 Tsukidate, where the world's largest horizontal acceleration was recorded, and two nearby points where high acceleration was also recorded, MYG012 Shioigama and MYG013 Sendai Oroshimachi. Figure 11 shows the acceleration waveforms at these three sites. At all three sites there were two distinct wave groups in the first and second halves, and the highest acceleration occurred in the second wave group. The pulses that generated the maximum accelerations were not just a single shot or two and have a certain length of duration; since their main frequencies were 5 Hz or more, it is suggested that these wave groups were generated from a small patch with an extremely high stress drop.

Investigation is currently ongoing as to the source of the observed strong-motion wave groups with many short-period components. While more details are likely to be forthcoming in the future, some of the latest findings are presented in the next section.

Before showing inverted strong motion generation areas, it would be worth to see how the wave packets were generated and propagated by lining up observed records in order of their observed locations (from north to south), which is quite informative. In Figure 12, the displacement and velocity waveforms of the EW components obtained by integrating the underground (borehole) records of KiK-net are lined up, considering the distance between the observation points to be the waveform interval and thereby synchronizing time. The figures show that seismic waves arrived earliest at MYGH08, which is located west of the epicenter, and it looks as if the seismic waves propagated from there to the north and south. Since the wave source was obviously near the hypocenter, not on land, they should not actually be straight lines, but they have been rendered as so in the figure for convenience.

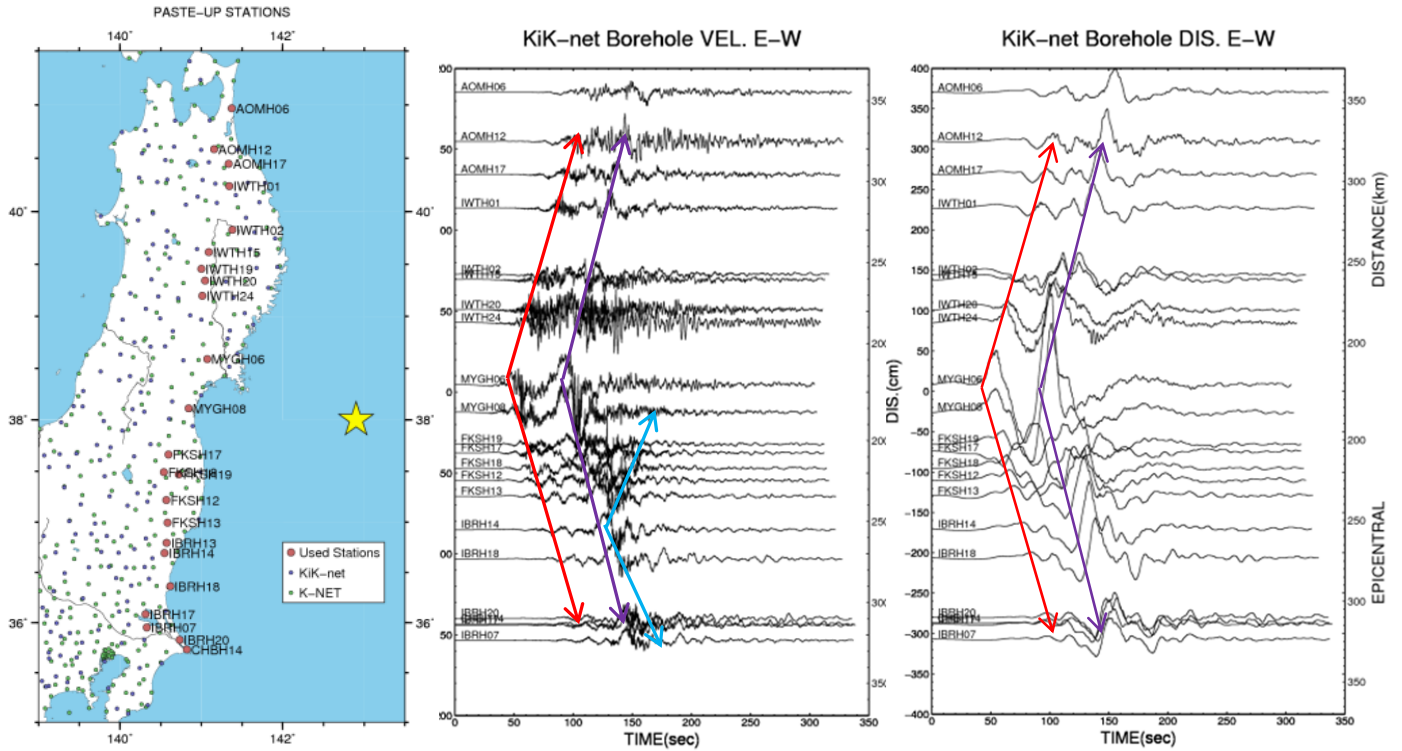


Figure 12. Paste-up of the velocity and displacement seismograms calculated from the borehole accelerograms of selected KiK-net data.

Looking at the displacement waveform, there is a time gap of approximately 50 seconds before the arrival of the second peak from the first one. The peak level is three times as high as that of the first wave group. Unlike the velocity waveform, the displacement waveform does not show the wave group that appears to have been generated in Fukushima Prefecture.

Likewise, the velocity waveform shows distinctly the first and second wave groups in Miyagi, Fukushima and Iwate Prefectures, along with the third wave group propagating from the south of Fukushima Prefecture. In the next section it shall be seen that focusing on this propagating wave packets allowed us the area that had generated short-period strong motions to be identified by its inversion to reproduce strong motions, and that the subsequent image of rupture process is turned out to be greatly different from that determined by the long-period seismic motions, crustal movement, and tsunami.

Lastly for this section, and in relation to the fact mentioned above, the interpretation of the difference from the well-established attenuation formula shall be discussed. In the attenuation formula shown in Fig. 10 the shortest distance to the fault plane was used as a representative distance. However, if short-period motions were not uniformly generated on the fault plane, the distance would be underestimated (i.e., shorter than reality) for those points located closer to the areas of the fault plane where short-period motions were not actually generated. If the area that generated strong motions has been identified, the representative distance should be the shortest distance to that area. As the simplest test for understanding such effects, we made a comparison between the observed PGAs and the empirical formula, assuming the simple distance to the hypocenter by JMA as the representative distance. Figure 13 shows that with a sufficiently long (~200 km) hypocentral distance, PGAs are no longer underestimated and the results are generally more consistent in distant areas. This indicates that the main energy of short-period motions came from the area or the areas that generated strong motions, not the whole fault plane equivocally. However, PGAs in the south side were relatively higher than those in the north side, indicating the presence of another area that generated strong motions in the south side, as shown in the next section for strong motion inversions.

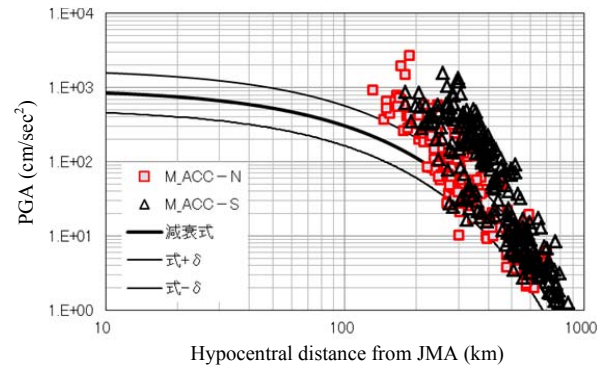


Figure 13. Observed PGAs versus simple hypocentral distances from the JMA hypocenter and the attenuation formula of Shi & Midorikawa (1999) in solid curves.

STRONG MOTION GENERATION AREAS

Strong motion seismology, an academic field that advanced rapidly after the 1995 Hyogo-ken Nanbu (Kobe) earthquake, tells us that slip distribution on a fault plane is quite heterogeneous and that the area that accumulates a large amount of strain, the so-called asperity, only occupies a small part of a fault plane. Its proportion is almost always consistent regardless of the scale of the fault size; in other words, an asperity can be scaled from the scale of the fault. In inland earthquakes, in most cases so far, the asperity that generates long-period (~several seconds) motions and the place that generates short-period motions, the so-called strong motion generation area (SMGA), roughly coincide with each other, or the asperity contains the SMGA.

Following the 2003 Tokachi-Oki Earthquake, some researchers suggested that these two may not necessarily be the same in large-scale ocean-trench earthquakes, but this idea has not been widely accepted.

The latest earthquake was large in scale and the area that generated long-period motions located near the ocean trench, about 100 km wide and 200 km long, coincided with the area with a high final slip obtained from tsunami and crustal movement with a longer time constant, and differences of the gross pictures among researchers were small as shown above. However, if a significant amount of short-period motions were also generated near the ocean trench, it would be difficult to explain why such strong short-period motions were generated as seen in Fig. 11 by such a shallow part of the fault, from which short-period motions must propagate over a long distance.

Asano and Iwata (2011) assumed that the first three wave groups in the observed waveform were emitted from different SMGAs and estimated the rupture initiation point for each SMGA using travel time analysis by identifying the first arrival of each wave group. As the result, the rupture initiation points (S1, S2, S3) of the SMGAs were determined to be at the locations indicated by stars in Fig. 14. The rupture starting times for S1, S2 and S3 were determined to be 25.0 s, 67.2 s, and 114.3 s, respectively.

They then performed waveform synthesis using empirical Green's function (0.1–10 Hz) to estimate the area, rise time, stress drop, rupture propagation velocity within SMGA and relative rupture initiation point within SMGA for SMGA1, 2 and 3 via grid search. Their targets were acceleration envelopes and displacement waveforms. The summation numbers of small earthquakes were determined by observed spectral ratio. EGF1, an aftershock that had occurred near the hypocenter, was used for SMGA1 and 2, and EGF2, an aftershock that had occurred near off Fukushima Prefecture, was used for SMGA3. The characteristics of the observed waveform were explained by this model. Their model explains acceleration waveforms, including PGAs, very well.

Likewise, Kawabe et al. (2011) identified SMGAs using empirical Green's function. They used the KiK-net (borehole) data for the Pacific coast to model SMGAs using forward modeling. The target frequency was 0.1–10 Hz, the same as that used by Asano and Iwata (2011), and the fault plane was assumed to be a rectangular plane that runs through the hypocenter announced by the JMA (strike 195°, dip: 13°) based on the shape of the Pacific Plate. For the empirical Green's function, the data of the Mj6.3 earthquake that occurred off Ibaraki Prefecture at 20:44 on October 19,

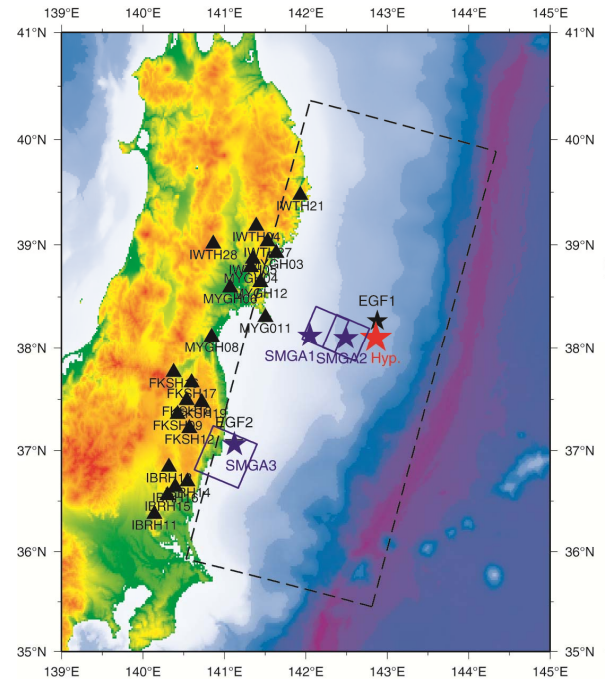


Figure 13. Strong motion generation areas based on the inversion for acceleration envelop and low-cut displacement seismograms by using empirical Green function method (Asano and Iwata., 2011).

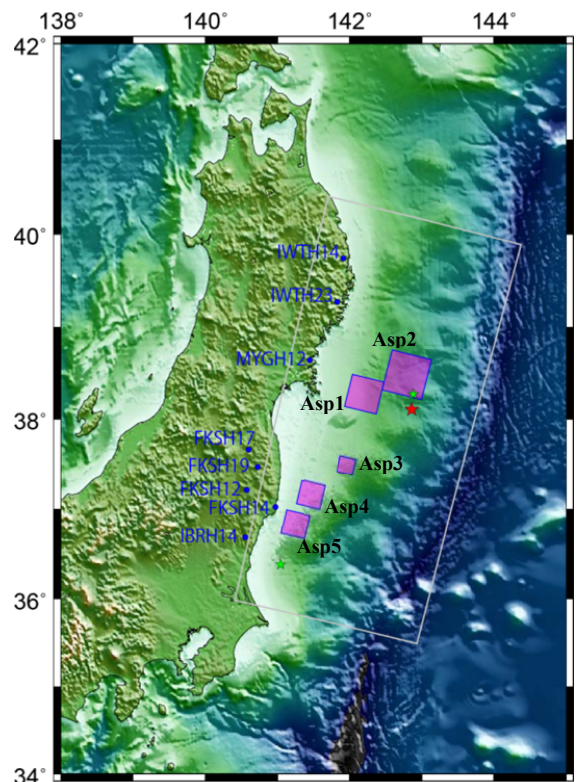


Figure 14. Strong motion generation areas obtained by Kawabe et al. (2011) by using the empirical Green function method.

2005, was used for Asp5 (SMGA) and the data of the Mj6.4 earthquake that occurred off Miyagi Prefecture at 3:16 on March 10, 2011, (an aftershock of the March 9 event) was used for all others.

First, they estimated the rupture process based on the propagation and arrival time of wave groups and other factors. They identified five wave groups and determined a SMGA for each. The results are shown in Fig. 14. Asp1 and Asp2 corresponded to SMGA1 and SMGA2 determined by Asano and Iwata (2011) and Asp5 corresponded to SMGA3. For Asp3 and Asp4, while it depends on how you look at the wave groups between them, at least there seems to be a clear necessity for the existence of Asp4 from looking at the paste-up of waveforms. Note that Kawabe et al. (2011) called them as asperities, but actually they obtained SMGAs if we should call the area with long-period, large slip near the Japan trench as the asperity of the main shock.

Kurahashi and Irikura (2011) also found five SMGAs, although at slightly different locations. Figure 15 shows their final source model that was derived from the observed strong motion accelerations and velocities of 14 KiK-net stations shown by red triangles. In this model they put three SMGAs around the hypocenter of the main shock. SMGA4 is similar to the SMGA3 of Asano and Iwata (2011).

We should note that the total seismic moments of these strong motion inversions are quite small; Asano and Iwata (2011) give $M_w=8.0$, Kawabe et al. (2011) $M_w=8.3$, and Kurahashi and Irikura (2011) $M_w=8.5$. This means these SMGA contributed only 3 to 18 % of the total seismic moment of this $M_w9.0$ event.

These specific concentrations of the short-period (less than a couple of seconds) strong motions in the regions close to the shore line are confirmed by the back projection analysis of teleseismic measurement by dense arrays in the US and Europe. For example, Dang and Mori delineated the movement of the energy release center as the peak point of the back projected coherent amplitude by using the US array. They carried out the back-projection analyses using data low-cut filtered at 1 second, band-passed filtered between 1 second and 5 seconds, and high-cut filtered at 5 seconds to find that short period motions are mainly generated from the deeper, western part of the fault plane, while long-period motions are from the middle of the fault plane.

SITE EFFECTS IN THESE AREAS

Site effect studies are intensively performed in the Tohoku region because of the subsequent moderate-size damaging earthquakes in the region after the advent of the K-NET and KiK-net as well as the JMA Shindokey network after the 1995 Kobe event. For example, back to 1998 Satoh et al. (1998) found K-NET site effect in the Tohoku region which can vary strongly from site to site. They found that at MYG005 (Onikobe) there is quite a large (~50) site amplification at around 0.7 Hz and at MYG013 (Sendai, Oroshimachi) a moderate (~10) amplification at the same frequency.

Later Kawase and Matsuo (2004) and Kawase (2006) used generalized spectral inversion by using YMGGH01 as a reference to obtain site amplification factors from the seismological bedrock (outcrop). Although amplifications at all the sites were not shown in these references, they also found quite a large amplification at several sites in the Tohoku region, especially in Miyagi and Iwate Prefectures. In Figure 16 horizontal and vertical site amplification factors at MYG004, MYG012 (Shiogama), and MYG013 relative to the seismological bedrock with the S wave velocity of 3.45km/s. Note that these site amplifications were determined by small to moderate ground motions, whose PGAs are all less than 200 Gals, observed from 1996 to 2002 or 2004. At MYG004 we can see a large amplification (~20) at around 10 Hz in the horizontal direction. As shown in the next section this peak were moved to lower frequency

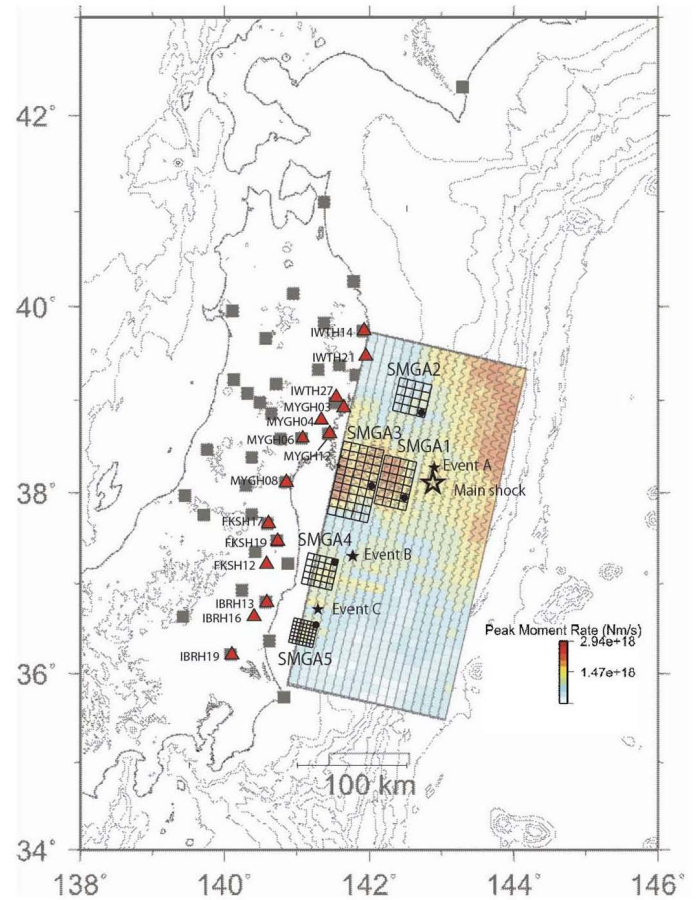


Figure 15. Strong motion generation areas obtained by Kurahashi and Irikura (2011) by using the empirical Green function method. Background contour is the distribution of peak moment-rate inverted using long-period strong motion data by Yoshida et al. (in preparation).

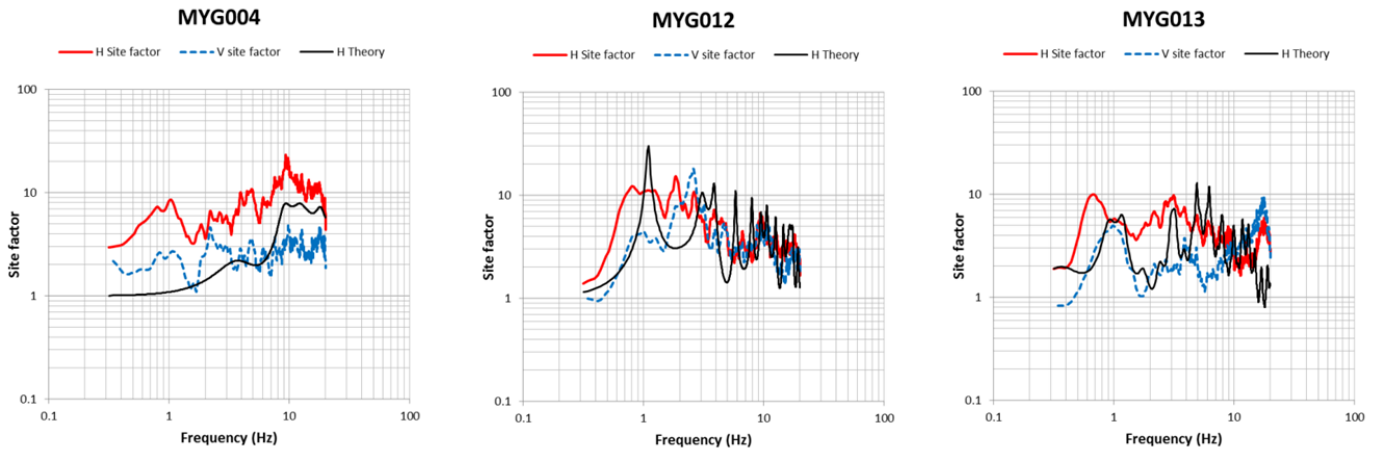


Figure 16. Site amplification factors determined by the generalized spectral inversion by Kawase and Matsuo (2004) and Kawase (2006) for three sites in Miyagi Prefecture for horizontal components (two components' RMS value) with red lines and vertical component with blue dotted lines. One-dimensional theoretical amplification characteristics for S-wave velocity structures taken from the PS logging for top 10 or 20 m and inverted by using genetic algorithm down to the bedrock are shown with black lines.

at around 5 Hz because of soil nonlinearity. There is a peak at around 1 Hz at MYG004, which does not have any corresponding peak in the theoretical prediction. We need to explore what kind of geological structure produces such a low-frequency peak. As for the sites MYG012 and MYG013 they also have peaks around 1 Hz or lower, however, they have corresponding peaks in the theoretical prediction, because of thick (0.5~1.5km) sedimentary rock formation in Pleistocene and Pliocene as derived by Satoh et al. (2001).

Here I would like to introduce specific information about the site conditions around MYG004 where the highest HPGA of 2.7g was observed. Photo 1 shows surrounding environment near the site. As we can see the station is close to the sharp slope of a small hill with a height of about 3 m. Thus there should be apparent 2D topographic effect for the site. As for the bedrock structure based on the PS logging data by NIED, it has only 4 m of sediments on top of the rock formation. That rock formation is weathered so that top 6.25 m has relatively low S-wave velocity as shown in Table 2. Apparently the top three layers of sediments should be the source of 10 Hz peak seen in Figure 16.

To delineate the effect of the small hill where the station rests, we measured microtremors along the line perpendicular to the direction of the hill axis, which is in the north-south direction. Figure 17 shows the spectral ratios of EW component (i.e., the direction of the hill axis) microtremors relative to the EW component of microtremor at the point 30m away from the foot of the hill. Z02 was placed in front of MYG004. As we can see from 10 Hz to 20 Hz, we have large amplification at Z01 and Z02, both of which are on the hill.



Photo 1. A small hill on which MYG004 K-NET Tsukidate site is situated. The direction of photo is from north northwest to south southeast. The flat part in front of the site is the parking lot of the Kurihara Cultural Hall (Bunka-Kaikan).

Table 2. Assumed structure as MYG004 model, whose S wave velocities are taken from those of MYG004 obtained from boring exploration up to 10 meters by NIED and inverted by Kawase and Matsuo (2004) and Kawase (2006) below 10 meters.

No.	density ρ (g/cm ³)	damping h	Thickness (m)	S wave velocity β (m/s)	P wave velocity α (m/s)
1	1.64	0.011	1.00	100	280
2	1.96	0.011	0.20	240	940
3	1.96	0.011	2.80	240	940
4	1.99	0.011	6.25	550	1800
5	2.18	0.011	20.00	1364	2729
6	2.37	0.011	110.00	2075	3594
7	2.54	0.011	50.00	2874	4978
8	2.67	0.011	∞	3400	5888

SOIL NONLINEARITY

Because of the strong ground motions soil nonlinearity inevitably has emerged in wide areas with high PGAs and PGVs and soft sediments. Notable damage were caused by the severe liquefaction, especially around the Tokyo Bay area where we have been making artificial land for quite a long time as deep as 50 m. Apparently the unprecedentedly long duration of strong motions in the area contribute the severe and pervasive liquefaction there. Unfortunately the author is not a specialist of liquefaction and so the report of observations and subsequent analyses are expected to be provided by other experts during this symposium. I only refer to the web pages of the Japanese Geotechnical Society related to liquefaction here (JGS, 2011).

I would like to show here some evidence of soil nonlinearity based on the horizontal-to-vertical (H/V) spectral ratios of strong motions during the Tohoku event. Figure 18 shows H/V ratios of the observed strong motions during the main shock and the 2005 Miyagi-ken Oki earthquake at MYG004 (NS component), MYG013 (NS component), and IBR002 (EW component), together with those calculated from the horizontal versus vertical site factors separated by Kawase and Matsuo (2004). The number in the top of each panel is the PGVs at these components during the main shock. As we can see at these site, the peak shift of H/V ratios are quite apparent and the degree of the shift seems to be depending on their PGV values. If PGV would be less than 30 cm/s, there seems no strong peak frequency shift in the H/V ratios. Since the main shock durations were as long as or more than 300 seconds, we may also see non-stationary characteristics of H/V ratios, which will be reported during the symposium. Since earthquake H/V ratios can be theoretically predicted by using the ratio of 1-D transfer function of vertically incident S-wave with respect to that of vertically incident P-wave, as long as the wave field is well diffused and consists mainly of body waves (Kawase et al., 2011), we could delineate the reduction levels of S wave velocity directly from these H/V ratios during the main shock.

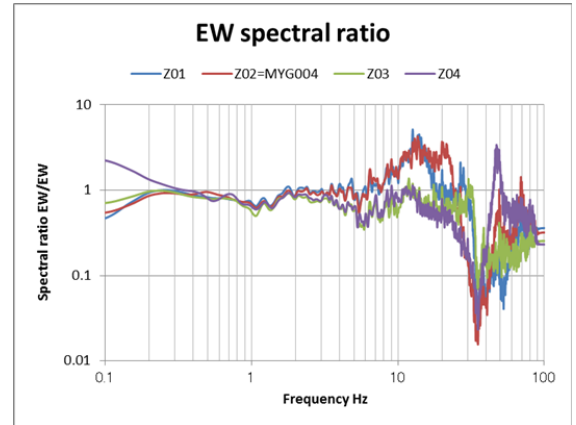


Figure 17. Spectral ratios of microtremors at four sensors deployed near the MYG004 K-NET Tsukidate. The direction of measured line is along the north-south direction perpendicular to the hill axis. Z01 and Z02 are on the hill, while Z03 and Z04 are on the flat part. The reference sensor is placed on the flat part 30 m away from the hill.

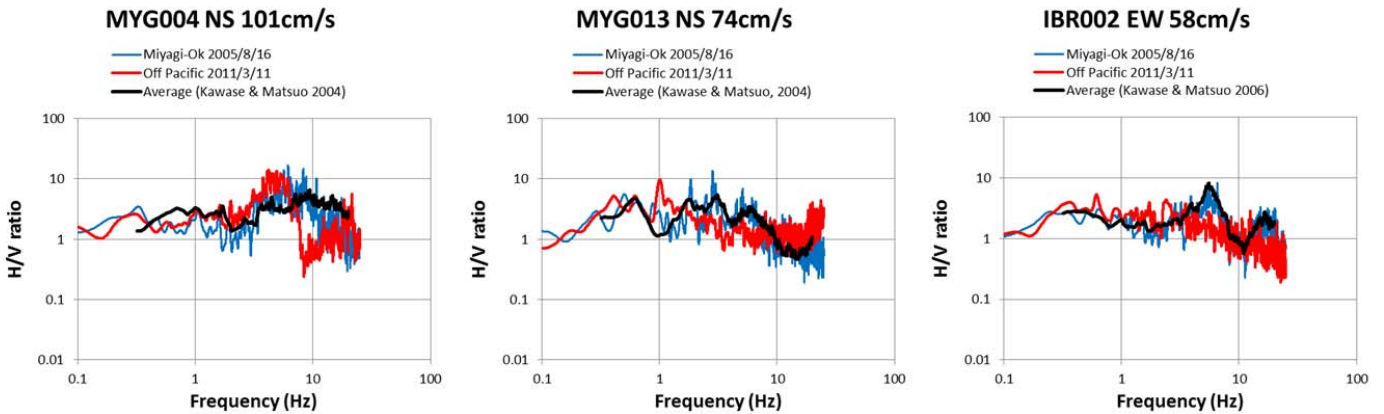


Figure 18. Horizontal-to-Vertical (H/V) spectral ratios for observed strong motions during the main shock (red lines) and the 2005 Miyagi-ken Oki earthquake (blue lines), together with the H/V ratios of the site factors determined by the generalized spectral inversion by Kawase and Matsuo (2004) for tens of weak to moderate ground motions .

LONG PERIOD MOTIONS

As expected long period motions were generated and propagating along the Japan's main island (Honshu), especially to the west because of the rupture directivity. However, based on the spectral shape of the observed strong motions in the Kanto Basin, there does not seem so much excitation of the basin-induced or basin-transduced surface waves in the long period range from 5 to 10 seconds as we have been observing in the previous earthquakes around the Kanto region. The durations of observed motions are quite long as expected but it is mainly a direct consequence of the large ruptured area and slow rupture propagation; that is, the source effect. These ground motions acted as input to high-rise buildings in Tokyo and Yokohama metropolitan areas and they produced quite large deformations, some of which can be seen as motion pictures on internet.

As for the long period motions we must mention about the conspicuously large ground motions at the ground floor and subsequent non-structural damage at one building in Osaka, Sakishima high-rise building now used as the Osaka Prefecture Government Office. Figure 19 show velocity seismograms and their Fourier spectra at the basement of the building on the reclaimed land in the Osaka Bay (by courtesy of Prof. Asano of DPRI, Kyoto Univ.) observed and released by Building Research Institute (BRI, 2011b). It shows quite a large amplitude at around 0.15 Hz. It is well known that in the coastal area of the Osaka Bay we can see large amplitude at around 4 to 6 seconds so that it is a serious question to engineers why they did not try hard to avoid resonance of the structure whose design period is said to be more than 5 seconds.

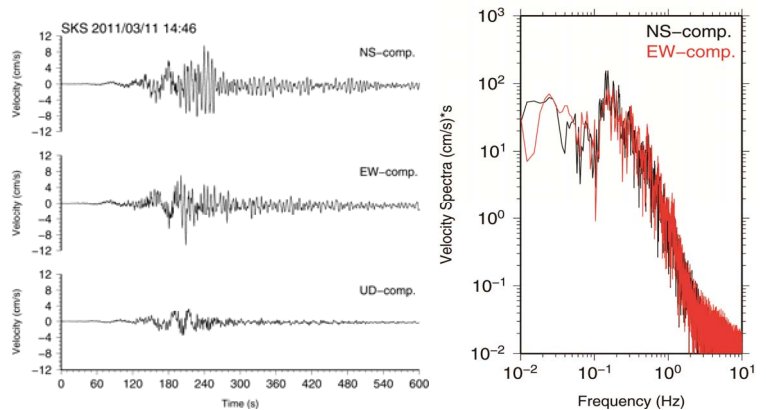


Figure 19. Three component velocity waveforms and their Fourier spectra of two horizontal components observed at the basement floor of the Sakishima Osaka Pref. Government Office. Building Research Institute installed the seismometers at the top, in the middle and at the basement (BRI, 2011b).

DAMAGE POTENTIAL OF THE OBSERVED STRONG MOTIONS

Structural damages caused by the strong ground motions were rather small, considering that PGAs of the strong motions generated in this earthquake was very high. For example, around the K-NET Tsukidate station (MYG004), where the highest acceleration of 2.7g was recorded, noticeable structural damages to buildings were difficult to confirm, except for the gymnasium of a nearby elementary school that had a minor damage in the non-structural elements. In this section, using the model developed by Nagato and Kawase (2004) for estimating heavy damages to mid- to low-rise reinforced concrete buildings, low-rise steel-frame buildings, and wooden houses to reproduce the damage ratios caused by the 1995 Hyogo-ken Nanbu earthquake, we shall estimate the structural damage potential of the observed strong motions and investigate the reason why the damages were relatively minor.

Figure 20 shows the estimated heavy-damage and collapse ratios calculated by inputting the observed strong motions from K-NET and KiK-net stations into the Nagato-Kawase Model. It can be seen that, with some exceptions, the damage ratio is lower than 10% at most points. While damage ratios of over 30% were estimated for several points with high acceleration, including K-NET Tsukidate, the estimated damage level was generally low.

The reason for this small damage potential of strong motions can be ascertained by approaching it from a different perspective. Figure 19 shows the diagram of PGA versus the equivalent predominant frequency, $PGA/2\pi PGV$, which has been used to examine the relationship between observed strong motions and structural damages. Equivalent predominant frequency is a simplified indicator of

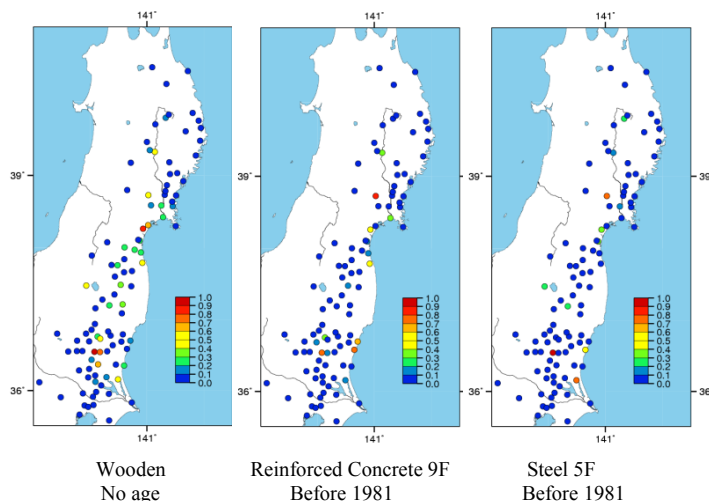


Figure 20. Estimated heavy damage or collapse ratios for observed strong motions by using Nagato and Kawase's (2004) damage prediction models.

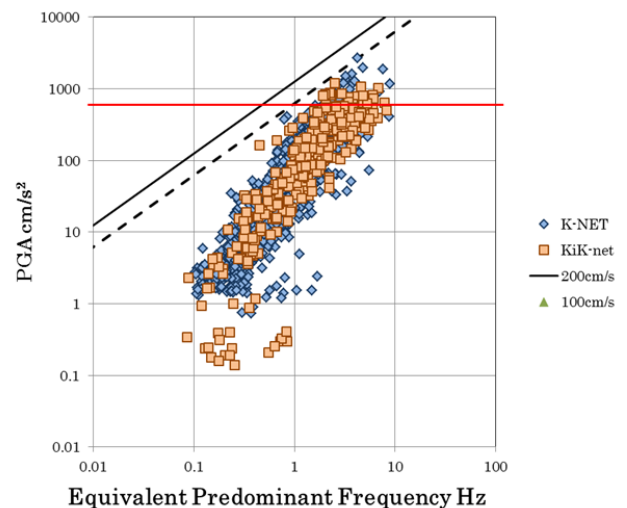


Figure 21. PGA and equivalent predominant frequency relationship. Symbols are K-NET and KiK-net data. Slant lines are equi-PGV lines.

the dominant frequency of seismic motions assuming sinusoidal nature. In this diagram equi-PGV lines will be a slope from left-down side to right-up side. The symbols are the observed values from K-NET and KiK-net data. The red line indicates 800 Gal and the dotted line indicates the uniform velocity line of 100 cm/s. These lines are considered to be danger lines based on the observation in Kobe, above which major damages are caused. The figure shows that the records with high PGAs all have a dominant frequency of 1 Hz or above and their PGVs are all lower than 100 cm/s (except for MYG004). Therefore, it is suggested that although the overall durations were much longer than those of the strong motions during the 1995 Hyogo-ken Nanbu Earthquake, the damages of the main shock were minor because the strong motions during the main shock were not dominant in the “moderately short-period” component around 1 second, which will cause heavy structural damages because they will give high PGAs and high PGVs at the same time.

SUMMARY

In this article, the data on the 2011 Off Pacific Coast of Tohoku, Japan Earthquake and its source characteristics as currently available were summarized, and the characteristics of the observed seismic motions and their structural damage potential were examined. As the Headquarters for Earthquake Research Promotion supposed to occur in near future, this earthquake had similar characteristics to the 1896 Meiji Sanriku-Oki Tsunami earthquake (i.e., a large slip occurring in a shallow area along the ocean trench, causing devastating tsunamis), and therefore generated a major slip causing a M9.0 earthquake. On the other hand, unlike usual tsunami earthquakes in this region that did not generate strong motions, this earthquake simultaneously generated rather strong, short-period dominant ground motions, which were generated in the areas deeper, closer to the land and does not coincide with the area that caused the M9.0 long-period slip. This came as no surprise, as it has always been pointed out that M7-class earthquakes in the Tohoku region, including the 1978 Miyagi-ken Oki earthquake of Mj7.8 and 2005 Miyagi-ken Oki earthquake of Mj7.4, would have short-period dominant motions. However, further studies are needed as to whether it is common or exceptional that a mega-thrust earthquake has always such a double face of a high stress event for strong motion generation and a slow slip event for tsunami generation.

With regards to site characteristics, the records show that significant nonlinearity was generated mainly at points where a high acceleration and/or velocity was recorded. It is clear that at K-NET Tsukidate (MYG004), where the highest acceleration of 2.7 g was recorded, topographic effects also played a role. It is expected that immense amounts of data obtained from this earthquake will greatly contribute to our further understanding of the surface geological effects of seismic motions.

The structural damage potential of this earthquake was by no means high when compared with inland crustal earthquakes such as the 1995 Hyogo-ken Nanbu earthquake. One of the reasons is that velocity pulses with a dominant frequency in the “moderately short-period” range (~ 1 second) were not generated, as these would have caused the severest damages to buildings. However, a large number of records with extremely high PGAs were obtained, and it is still an issue why major damage was not created at such high acceleration levels, an examination of which must include the evaluation of the actual seismic resistance of Japanese buildings.

ACKNOWLEDGEMENT

Microtremor observations at MYG004 were performed by the joint investigation team of DPRI (H.K, S. Matsushima, Baoyintu, F. Nagashima, K. Nakano) and Shimizu Corp. (T. Satoh, T. Hayakawa, M. Ohshima). Data from K-NET and KiK-net distributed promptly by NIED are highly appreciated. Thanks are also given to Profs. K. Irikura, H. Kawabe, and K. Asano for their kind and prompt supply of their unpublished materials and to all the institutions who provided us their nice scientific findings on the web.

REFERENCES

- Asano, K. and T. Iwata [2011], <http://sms.dpri.kyoto-u.ac.jp/k-asano/pdf/jpgu2011.pdf>
- Building Research Inst. [2011a], http://iisee.kenken.go.jp/staff/fujii/OffTohokuPacific2011/tsunami_ja.html
- Building Research Inst. [2011b], http://www.kenken.go.jp/japanese/contents/topics/20110311/pdf/quickreport/0311quickreport_40.pdf
- Earthquake Research Inst. [2011], http://outreach.eri.u-tokyo.ac.jp/eqvolc/201103_tohoku/danwakaishiryou/
- The Geospatial Information Authority of Japan [2011a], <http://www.gsi.go.jp/cais/topic110314.2-index.html>
- The Geospatial Information Authority of Japan [2011b], <http://www.gsi.go.jp/cais/topic110520-index.html>

- The Headquarters for Earthquake Research Promotion [2009], http://www.jishin.go.jp/main/chousa/09mar_sanriku/f01.htm
- The Japanese Geotechnical Society, [2011], http://www.jiban.or.jp/index.php?option=com_content&view=article&id=1073&Itemid=29
- Japan Meteorological Agency [2011a], <http://www.mri-jma.go.jp/Dep/sv/2011tohokutaiheiyo/index.html>
- Japan Meteorological Agency [2011b], http://www.seisvol.kishou.go.jp/eq/daily_map/sendai/20110311.shtml
- Japan Meteorological Agency [2011c], http://www.seisvol.kishou.go.jp/eq/daily_map/sendai/20110309.shtml
- Kawabe, H. et al. [2011], <http://www.rri.kyoto-u.ac.jp/jishin/>
- Kawase, H. and H. Matsuo [2004], “Amplification Characteristics of K-NET, Kik-NET, and JMA Shindokey Network Sites Based on the Spectral Inversion Technique”, *13th World Conference on Earthquake Engineering*, Vancouver, Canada, Paper No. 454.
- Kawase, H. [2006], “Site Effects Derived From Spectral Inversion Method for K-NET, Kik-Net, and JMA Strong-Motion Network with Special Reference to Soil Nonlinearity in High PGA Records”, *Bull. Earthq. Res. Inst., Univ. Tokyo*, **81**, 309-315.
- Kawase, H., F. J. Sánchez-Sesma, and S. Matsushima [2011], “The Optimal Use of Horizontal-To-Vertical Spectral Ratios of Earthquake Motions for Velocity Inversions Based on Diffuse Field Theory for Plane Waves”, *Bull. Seism. Soc. Am.*, **101** (in press).
- Kurihashi, S. and K. Irikura [2011], Source model for generating strong ground motions during the 11 March 2011 off Tohoku, Japan earthquake, EPS, Special Issue (in print).
- Nagato, K. and H. Kawase, [2004], Damage Evaluation Models of Reinforced Concrete Buildings Based on the Damage Statistics and Simulated Strong Motions During the 1995 Hyogo-ken Nanbu Earthquake, *Earthquake Engineering and Structural Dynamics*, Vol.33, No.6, 755-774, 2004.6.
- National Inst. Earth Science and Disaster Prevention, [2011], http://www.kyoshin.bosai.go.jp/kyoshin/topics/TohokuTaiheiyo_20110311/nied_kyoshin2j.pdf
- Satoh, T., H. Kawase, and S. Matsushima [1998], Source Spectra, Attenuation Function, and Site Amplification Factors Estimated from the K-NET Records for the Earthquakes in the Border of Akita and Miyagi Prefectures in August, 1996, Zisin, Journal of the Seismological Society of Japan, Series-2, 50, No.4, 415-429.
- Satoh, T., H. Kawase, and S. Matsushima [2001], Estimation of S-wave velocity structures in and around the Sendai Basin, Japan, using array records of microtremors, *Bulletin of the Seismological Society of America*, 91, 206-218.
- Shi S. and S. Midorikawa [1999], New Attenuation Relationships for Peak Ground Acceleration and Velocity Considering Effects of Fault Type and Site Condition, *J. of Struct. Constr. Eng.*, Architectural Institute of Japan, 523, 63-70.
- Wang D. and J. Mori [2011], Rupture Process of the 2011 off the Pacific Coast of Tohoku Earthquake (Mw 9.0) as Imaged with Back-Projection of Teleseismic P-waves, EPS, Special Issue (in print).